

1 **Supplementary Material:**

2

3 **Mixing state of individual submicron carbon-containing particles**
4 **and their seasonal variation in urban Guangzhou, China**

5

6 Guohua Zhang^{1,2}, Xinhui Bi^{1,*}, Lei Li³, Lo Yin Chan¹, Mei Li³, Xinming Wang¹,

7 Guoying Sheng¹, Jiamo Fu^{1,3}, Zhen Zhou³

8

9 1. State Key Laboratory of Organic Geochemistry, Guangzhou Institute of

10 Geochemistry, Chinese Academy of Sciences, Guangzhou 510640, P. R. China

11 2. Graduate University of Chinese Academy of Sciences, Beijing 100039, P. R.

12 China

13 3. School of Environmental and Chemical Engineering, Shanghai University,

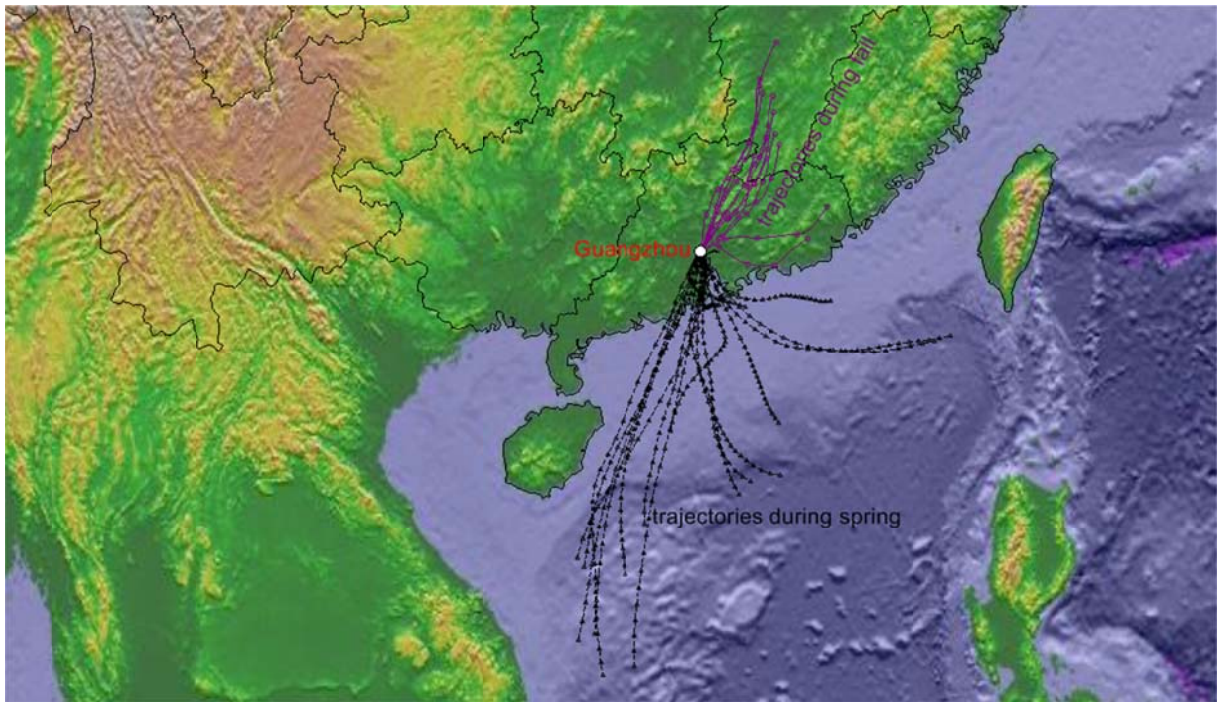
14 Shanghai 200444, P. R. China

15

16 Correspondence to: Xinhui Bi (bixh@gig.ac.cn)

17 Tel: +86-20-85290195

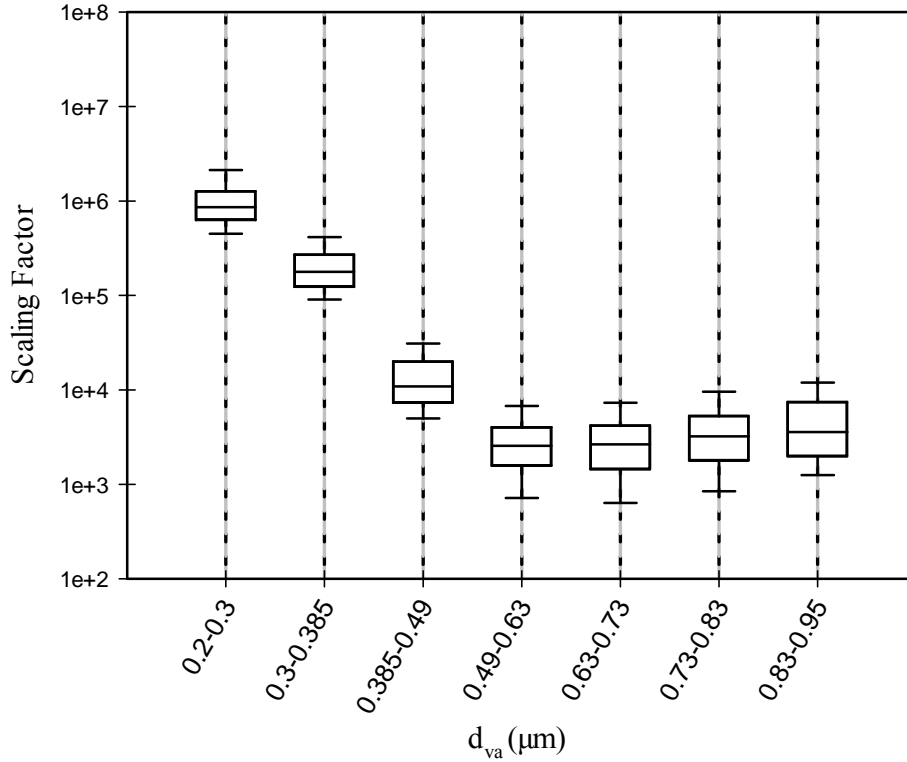
18 Fax: +86-20-85290288



20

21

24 **Fig. S1.** Daily backward air-mass trajectories reaching urban Guangzhou site ending
25 at 500 m above sea level and 0: 00 (local time) during spring and fall sampling
26 periods.



24

25

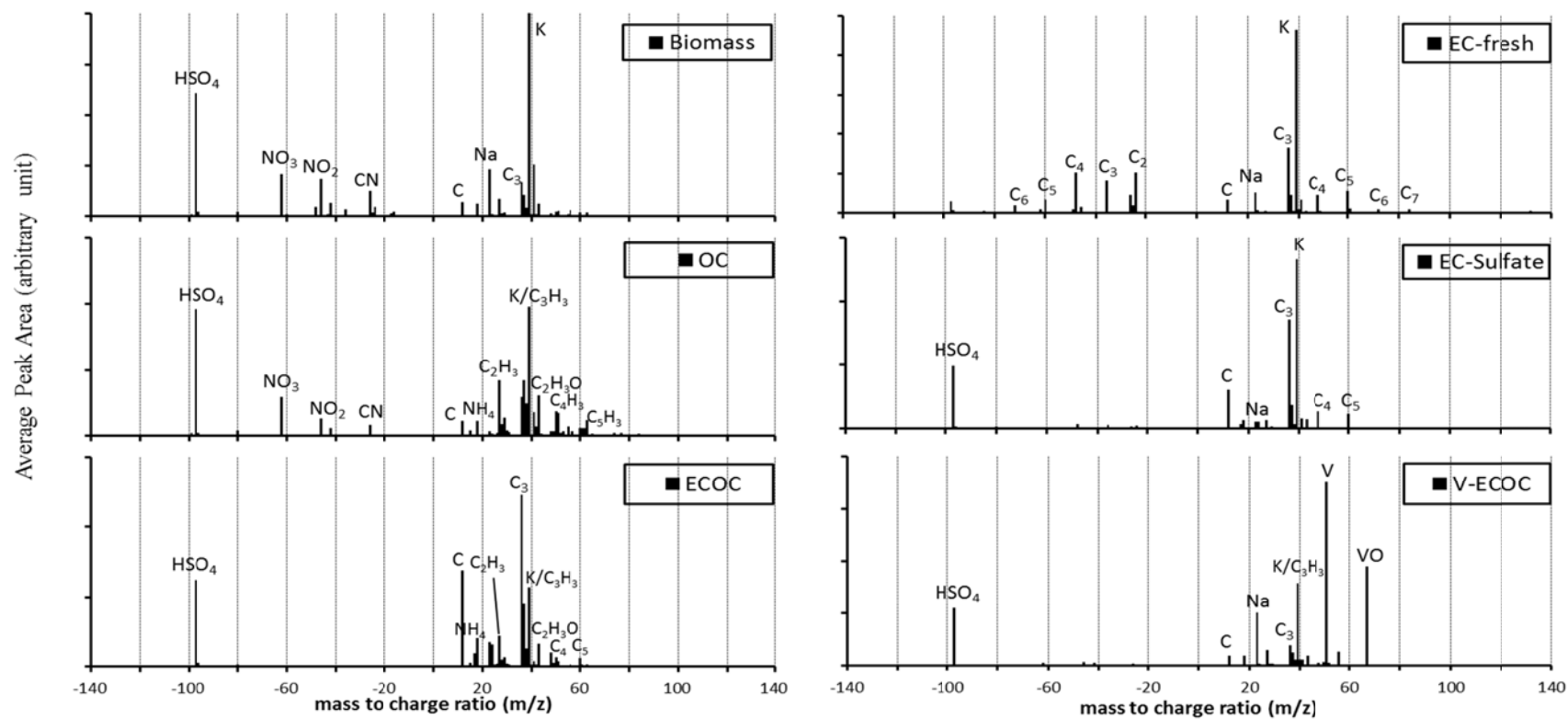
26 **Fig. S2.** Box-whisker plots of SPAMS scaling factor using SMPS + C for Spring
 27 period 2010 in Guangzhou. The median (line in the box), quartile (box), 10% and 90%
 28 percentile (whiskers) were shown. The size-dependence pattern of the scaling factor is
 29 similar to those described in earlier studies with single particle mass spectrometry
 30 (Healy et al., 2012; Jeong et al., 2011).

31 Scaling procedure for SPAMS data: firstly, the conversion of d_m to d_{va} was
 32 performed according to the methodology described by (DeCarlo et al., 2004):

$$33 \quad d_{va} = \rho_p / \rho_0 \times d_{ve} / \chi$$

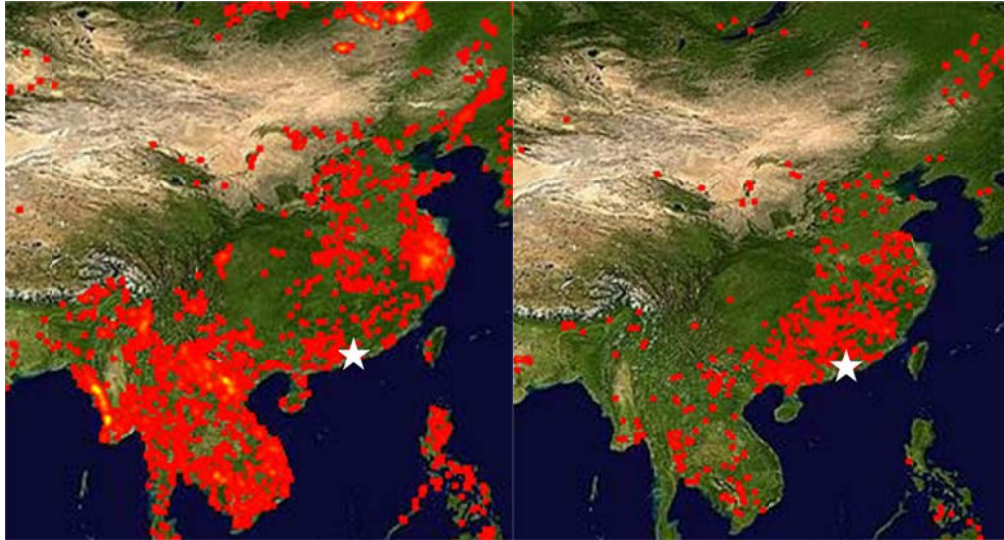
34 where ρ_p is the particle density, ρ_0 is standard density (1 g cm^{-3}), d_{ve} is particle
 35 volume equivalent diameter, and χ is the dynamic shape factor (assumed to be 1). All
 36 particles were assumed to be spherical with no internal voids, thus d_m is equal to d_{ve} .

37 A single density value of 1.7 g cm^{-3} (Cheng et al., 2006) was chosen to convert the d_m
38 to d_{va} . Certain error might also be introduced based on the usage of an assumed
39 density for scaling process, while previous work has attained satisfactory results
40 (Healy et al., 2012; Reinard et al., 2007). Secondly, the particle size range from
41 SPAMS was divided into seven size bins (0.2-0.3, 0.3-0.39, 0.39-0.49, 0.49-0.63,
42 0.63-0.73, 0.73-0.83 and 0.83-0.95 μm), corresponding to seven size bins from SMPS
43 + C created by merging adjacent pairs of size bins, approximately covering a d_m size
44 range of 124-521 nm (mid-point). Thirdly, scaling factor was calculated for each size
45 bin through dividing the size-segregated hourly average number concentration from
46 SMPS + C by the simultaneously observed hourly total SPAMS particle number count
47 in the corresponding size bin (Rehbein et al., 2012). The hourly scaling factors in each
48 size range were utilized in scaling the number concentration of particles by directly
49 multiplying SPAMS counts of each single particle type of the exactly same size range
50 in that hour.



61

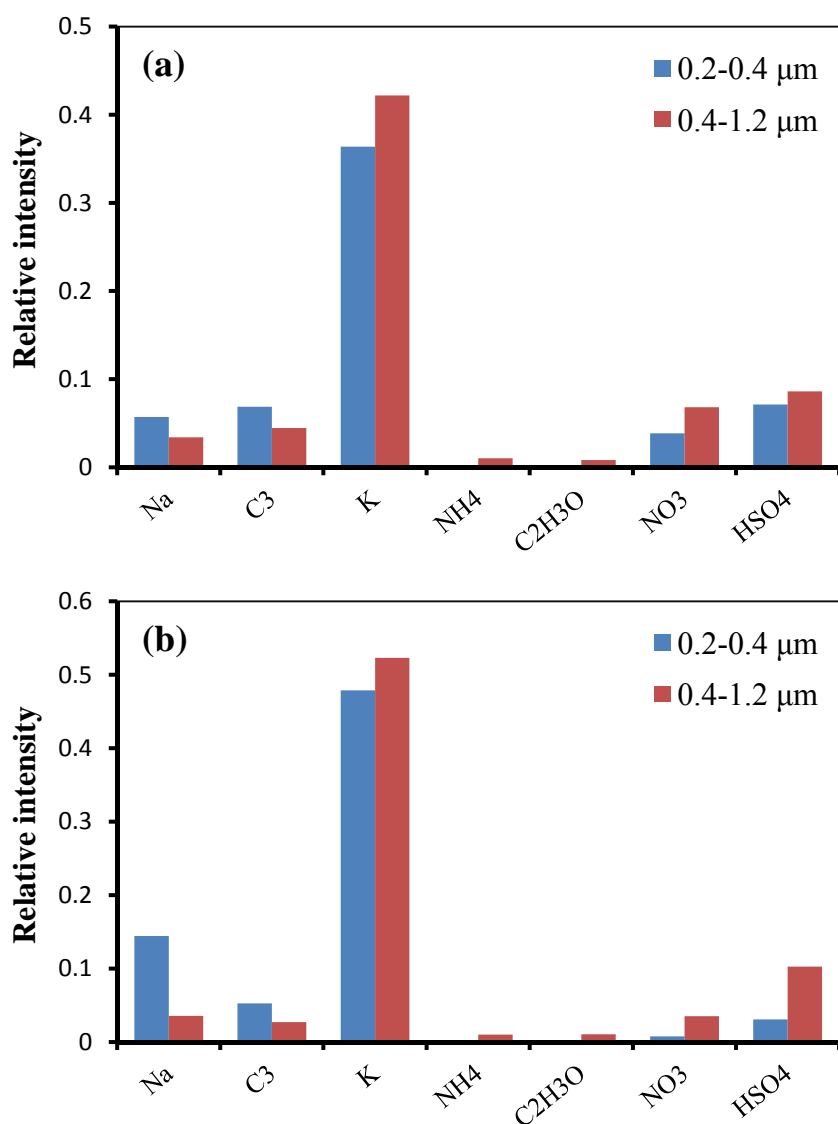
62 **Fig. S3.** Averaged positive and negative mass spectra for the 6 single particle carbon-containing classes observed during the fall sampling period.



64

65

70 **Fig. S4.** Fire maps from MODIS on board the Terra and Aqua satellites during
71 2010/05/01-2010/05/10 (left), and 2010/11/07-2010/11/16 (right). The fire map
72 accumulates the locations of the fires over a 10-day period. Each colored dot indicates
73 a location where MODIS detected at least one fire during the compositing period. The
74 star marker signifies the location of sampling site.



70

71

72 **Fig. S5.** Comparison of relative intensity for different species in smaller (0.2-0.4 μm)

73 and larger (0.4-1.2 μm) Biomass particles during spring (a) and fall period (b),

74 respectively.

75

76 **References**

- 77 Cheng, Y. F., Eichler, H., Wiedensohler, A., Heintzenberg, J., Zhang, Y. H., Hu, M.,
78 Herrmann, H., Zeng, L. M., Liu, S., and Gnauk, T.: Mixing state of elemental carbon and
79 non-light-absorbing aerosol components derived from in situ particle optical properties
80 at Xinken in Pearl River Delta of China, *J. Geophys. Res.*, 111, D20204, 2006.
- 81 DeCarlo, P. F., Slowik, J. G., Worsnop, D. R., Davidovits, P., and Jimenez, J. L.: Particle
82 morphology and density characterization by combined mobility and aerodynamic
83 diameter measurements. Part 1: Theory, *Aerosol Sci. Tech.*, 38, 1185-1205, doi:
84 10.1080/027868290903907, 2004.
- 85 Healy, R. M., Sciare, J., Poulain, L., Kamili, K., Merkel, M., Müller, T., Wiedensohler, A.,
86 Eckhardt, S., Stohl, A., Sarda-Estève, R., McGillicuddy, E., O'Connor, I. P., Sodeau, J.
87 R., and Wenger, J. C.: Sources and mixing state of size-resolved elemental carbon
88 particles in a European megacity: Paris, *Atmos. Chem. Phys.*, 12, 1681-1700, doi:
89 10.5194/acp-12-1681-2012, 2012.
- 90 Jeong, C. H., McGuire, M. L., Godri, K. J., Slowik, J. G., Rehbein, P. J. G., and Evans, G. J.:
91 Quantification of aerosol chemical composition using continuous single particle
92 measurements, *Atmos. Chem. Phys.*, 11, 7027-7044, doi: 10.5194/acp-11-7027-2011,
93 2011.
- 94 Rehbein, P. J. G., Jeong, C.-H., McGuire, M. L., and Evans, G. J.: Strategies to Enhance the
95 Interpretation of Single-Particle Ambient Aerosol Data, *Aerosol Sci. Tech.*, 46, 584-595,
96 doi: 10.1080/02786826.2011.650334, 2012.
- 97 Reinard, M. S., Adou, K., Martini, J. M., and Johnston, M. V.: Source characterization and

98 identification by real-time single particle mass spectrometry, *Atmos. Environ.*, 41,
99 9397-9409, doi: 10.1016/j.atmosenv.2007.09.001, 2007.